water

MDPI

Article

Spatial Composition of Flood-Disturbance Forcing and Changes in the Abundance of Aquatic Organisms Before and After Floods in Channelized Streams

Koji Hijikata [1,2,*] and Morihiro Harada [3]

[1] Department of Engineering Science, Gifu University, 1-1, Yanagido, Gifu 501-1193, Japan
[2] Dainichi Consultant Inc., 3-1-21, Yabutaminami, Gifu 500-8384, Japan
[3] Center for Environmental and Societal Sustainability, Gifu University, 1-1, Yanagido, Gifu 501-1193, Japan; harada.morihiro.i3@f.gifu-u.ac.jp
* Correspondence: hijikata-k@dainichi-consul.co.jp; Tel.: +81-58-271-2501

Abstract

Flow velocity and bed shear stress are spatially heterogeneous during floods. Although flow refugia and flood responses have been studied, relationships between proportions of areas exposed to different levels of flood-disturbance forcing and changes in the abundance of aquatic organisms remain unclear. We examined these relationships and implications for channel design across nine reaches of three channelized cobble-bed streams during two floods in one year. Percentage changes were calculated from flow-corrected environmental DNA (eDNA) rates for three fish species and densities for two benthic macroinvertebrate life types. Two-dimensional modeling estimated peak-flood velocity and bed shear stress. Grid cells were classified by forcing level using swimming ability and bed-material movement thresholds; proportions of low- and high-disturbance areas (LDA and HDA) were calculated within whole and normal-flow channels. Linear mixed-effects models examined associations while accounting for flood event and repeated observations within reaches. Positive coefficients were estimated for Dark chub and Pale chub with whole-channel velocity-based LDA, and a negative coefficient for net-spinners with normal-flow-channel shear-stress-based HDA. Unadjusted *p*-values were below 0.05 for Pale chub and net-spinners, but no disturbance-area coefficient remained significant after Benjamini–Hochberg correction across 32 models. Although ecological validation is needed, these exploratory findings may inform channel design.

Keywords: flood disturbance; flow refugia; spatial heterogeneity; environmental DNA; benthic macroinvertebrates; two-dimensional flow modeling; channelized streams

Academic Editor: Michele Mistri

Received: 9 October 2026
Revised: 5 November 2026
Accepted: 12 November 2026
Published: 16 November 2026

Copyright: © 2026 by the authors. Licensee MDPI, Basel, Switzerland. This article is an open access article distributed under the terms and conditions of the Creative Commons Attribution (CC BY) license.

1. Introduction

Floods are one of the major natural disturbances shaping river morphology and biological communities, and riverine organisms exhibit diverse adaptations to natural flow variability, including floods [1,2]. During floods, increases in flow velocity and bed shear stress can cause the downstream displacement of aquatic organisms, bed-material movement, and habitat destabilization, thereby reducing biological abundance after floods [3,4]. Therefore, understanding changes in the abundance of aquatic organisms before and after floods requires consideration not only of flood magnitude, such as peak discharge,

but also of the physical forcing exerted on aquatic organisms within the channel during floods, including flow velocity and bed shear stress.

Physical forcing during floods is not spatially uniform within a channel but varies with channel morphology, bed material, vegetation, and other local conditions. Lancaster and Hildrew [5] showed that areas exposed to relatively weak forcing can persist even under high-flow conditions and may function as flow refugia. Bed-material movement is also spatially heterogeneous, with stable and strongly disturbed patches coexisting as a mosaic [6]. Hydraulic conditions and the potential function of refugia also vary with location within the channel [7,8]. These findings indicate that physical forcing during floods should be evaluated not only using reach-averaged flow velocity or bed shear stress, but also in terms of the spatial composition of areas exposed to different levels of forcing within the channel.

Furthermore, the biological significance of this spatial composition is likely to differ among organisms depending on their mobility and life type. Fish are known to use low-velocity areas along channel margins and in lateral channel areas during floods, and swimming ability and broader-scale movement are also related to their responses to high flows [9–11]. Thus, for fish, physical conditions may be relevant not only within the normal-flow channel but also in lateral channel areas newly inundated during floods. In contrast, for benthic macroinvertebrates inhabiting the bed surface or interstitial spaces, bed shear stress and bed-material movement are related to habitat stability, while mobility and resistance strategies during floods differ among life types [4,8]. In particular, for organisms that live attached to or settled on the substrate, changes in abundance may be related to the forcing acting on the bed within the normal-flow channel. Thus, when relating flood-disturbance forcing to changes in the abundance of aquatic organisms, it is important to consider not only the type of forcing but also whether that forcing is evaluated across the whole channel inundated during floods or only within the normal-flow channel.

Considering both the type of forcing and the area of the channel evaluated may be particularly important in channelized streams. Channel modification for flood protection, land use, and other purposes has been widely reported to simplify channel morphology and reduce physical heterogeneity and habitat diversity [12,13]. Channel morphology can influence the spatial heterogeneity of flow velocity and bed shear stress during floods and the availability of potential flow refugia [14], whereas restoring structural heterogeneity does not necessarily produce clear responses in fish or benthic macroinvertebrates [13]. In Japanese streams, channel modification has often produced narrow, deep cross sections and morphologically uniform channels [15,16], making channelized streams an important setting in which to examine these relationships.

Previous studies have examined biological responses to floods using habitat classifications, such as riffles, pools, backwaters, and inundated areas, as well as observations of fish movements, flow-refugia use, benthic macroinvertebrate drift, and changes in local abundance [4,7–9,11]. These approaches provide valuable ecological insights. However, habitat classifications alone do not directly quantify hydraulic forcing during floods, and observed fish movements, flow-refugia use, and changes in abundance cannot always be readily predicted for proposed channel configurations at the planning and design stage. In contrast, flow velocity and bed shear stress can be estimated from discharge and channel geometry using hydraulic models, providing potential measures for evaluating flood-time conditions under different channel configurations [14]. However, their ecological relevance cannot be established from hydraulic calculations alone. In particular, the relationships between the spatial proportions of areas exposed to different levels of flow velocity or bed shear stress within the whole or normal-flow channel and observed changes in abundance before and after floods remain insufficiently examined. We therefore

hypothesized that the spatial composition of flood-disturbance forcing would be associated with changes in the abundance of aquatic organisms before and after floods.

To test this hypothesis, we analyzed the relationship between the spatial composition of flood-disturbance forcing and changes in the abundance of aquatic organisms before and after two flood events in June and August 2024 across nine study reaches in three channelized cobble-bed streams. Our objective was to examine how the proportions of low- and high-disturbance areas, defined using flow velocity and bed shear stress within the whole or normal-flow channel, corresponded to changes in abundance in each organism group, and to explore the potential application of these hydraulically estimable indicators to channel planning and design.

2. Materials and Methods

2.1. Study Area and Flood Events

2.1.1. Study Rivers and Reaches

This study was conducted in three tributaries of the Tsubo River in the Kiso River system in central Honshu, Japan: the Kawaura, Nakanoho, and Mugikura Rivers (Figure 1). All three are channelized cobble-bed streams with revetments along both banks. The Nakanoho and Mugikura Rivers flow mainly through valley-bottom plains, whereas the Kawaura River flows from a valley-bottom plain onto an alluvial fan.

In each river, two reaches with alternate bars and one reach with a flat bed were selected, resulting in a total of nine study reaches. Each study reach was approximately 100 m long, and reaches within the same river were separated by at least 1 km. Across the nine reaches, channel width ranged from approximately 13 to 46 m, bed slope from 1/120 to 1/67, and the representative grain size, d60, from 50 to 80 mm (Table 1). The length of each study reach corresponded to approximately 2–8 times the channel width and was classified as the channel-unit scale according to the spatial-scale classification of Nagayama et al. [17].

Table 1. Channel characteristics and peak discharges at the nine study reaches.

Item		Study Reach								
		Kawa -ura1	**Kawa -ura2**	**Kawa -ura3**	**Naka -noho1**	**Naka -noho2**	**Naka -noho3**	**Mugi -kura1**	**Mugi -kura2**	**Mugi -kura3**
Average channel width (m)		46.63	22.56	19.30	17.12	13.02	17.41	17.69	18.10	12.78
Channel slope (1/X)		108	95	95	67	90	95	87	120	100
Representative grain size, d_{60} (mm)		75	65	70	52	80	80	50	55	55
Discharge (m^3/s)	June Flood	61	56	47	32	21	18	16	9	6
	August Flood	60	50	41	24	19	14	16	9	6

Note: d_{60} denotes the grain size for which 60% of the bed material is finer by weight. June and August denote the 2024 flood events.

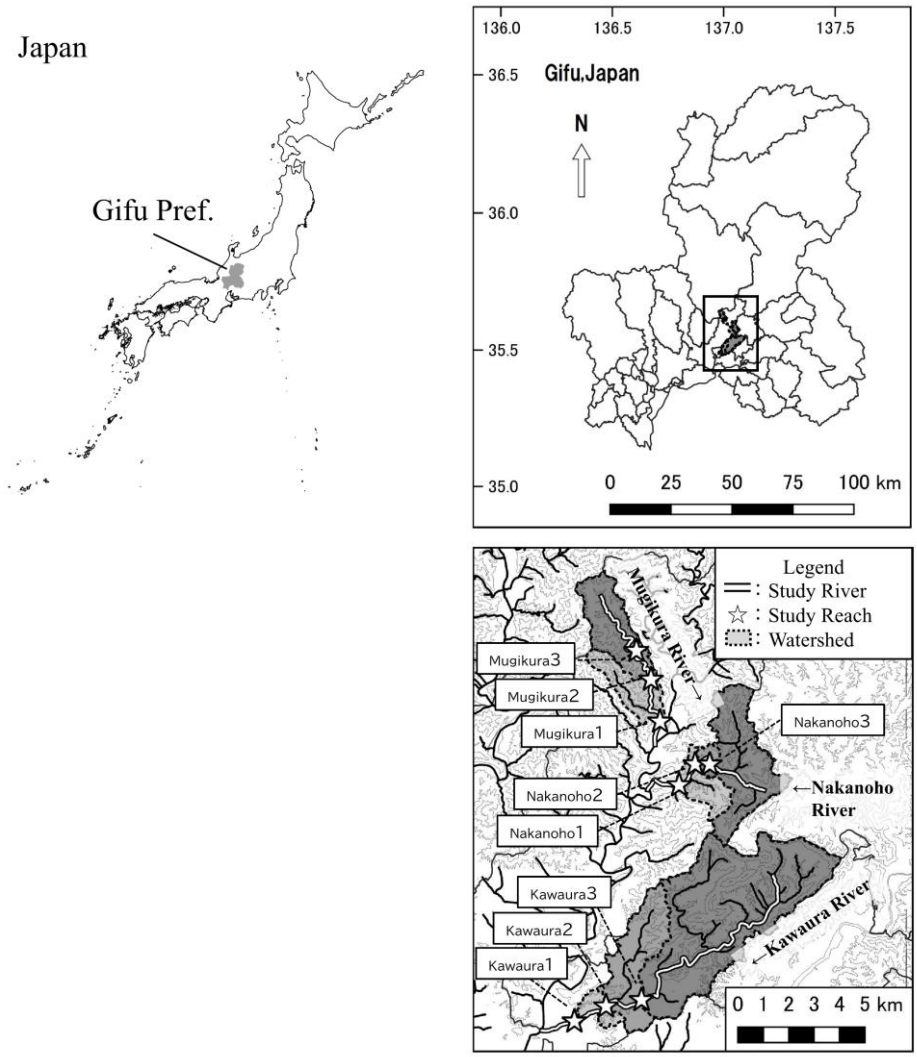


Figure 1. Locations of the study rivers and study reaches in the Tsubo River basin, Kiso River system.

2.1.2. Study Period and Flood Events

The study period extended from May to October 2024, covering the rainy season through the typhoon season. We focused on two flood events that occurred during this period: a flood associated with the rainy-season front in late June (hereafter, the June flood event) and a flood associated with Typhoon No. 10 in late August (hereafter, the August flood event) [18,19]. Peak discharge ranged from 6 to 61 m^3/s during the June flood event and from 6 to 60 m^3/s during the August flood event, and peak discharges at each study reach were generally similar between the two events.

Benthic macroinvertebrate and fish surveys were conducted before and after each flood event, using the most recent survey before each event as the pre-flood survey. For the June flood event, pre-flood surveys were conducted on 17–19 June, the flood peaked on 23 June, and post-flood surveys were conducted on 27 June. For the August flood event, pre-flood surveys were conducted on 20–22 August, the flood peaked on 31 August, and post-flood surveys were conducted on 6 September. The intervals between the pre- and post-flood surveys were 8–10 days for the June event and 15–17 days for the August event. The post-flood surveys were conducted approximately four and six days after the respective flood peaks, once the increased flows had subsided sufficiently to allow access to the channel. Surveys within each river were completed within a single day. The discharge hydrographs and timing of the biological surveys for each river are shown in Figure 2.

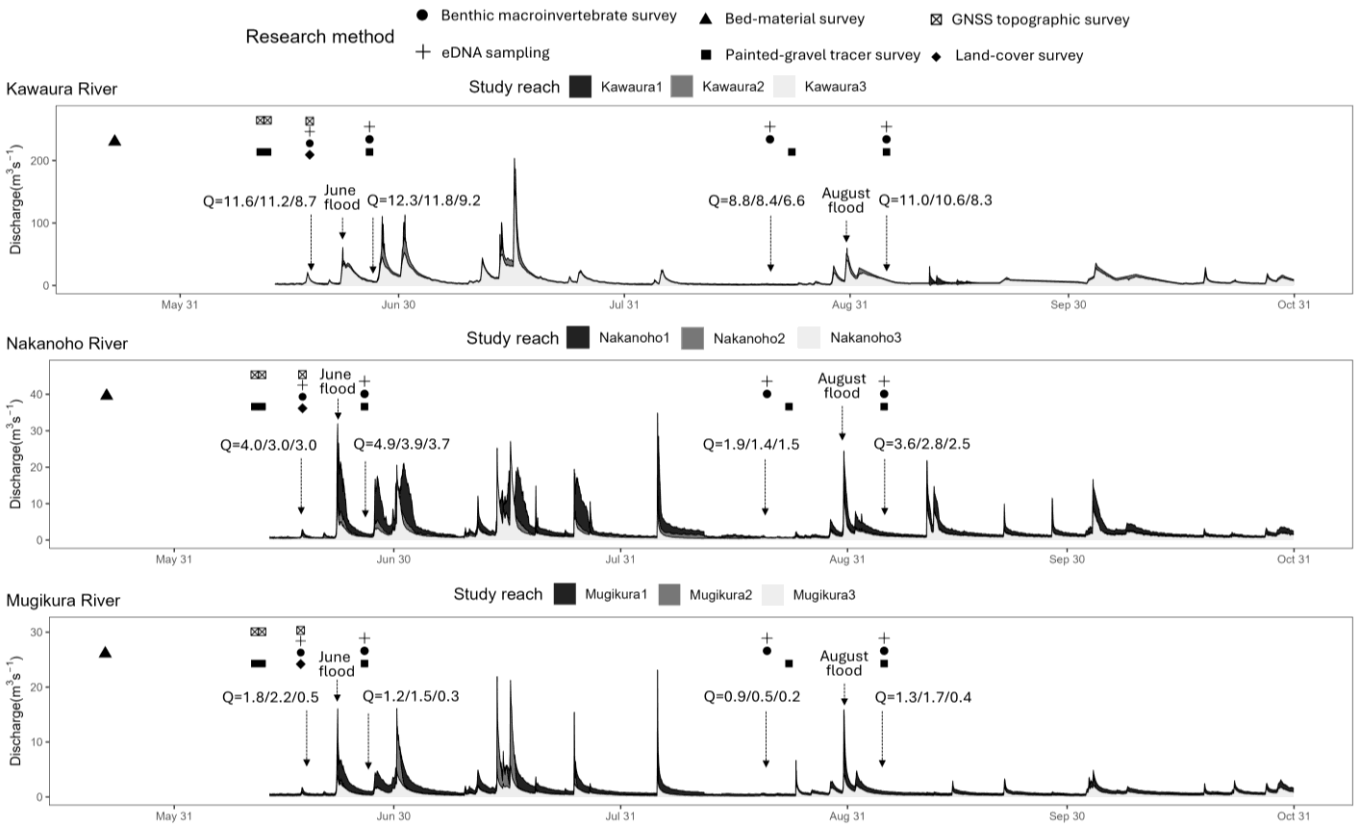


Figure 2. Discharge hydrographs and timing of biological surveys for the June and August 2024 flood events in the three study rivers.

2.2. Biological Surveys and Calculation of Response Variables

The overall survey and analysis workflow is shown in Figure 3.

2.2.1. Benthic Macroinvertebrate Survey

For the benthic macroinvertebrate survey, quantitative sampling using the kick-sweep method was conducted at three sites representing typical habitat conditions within each study reach. A 0.5 × 0.5 m quadrat was established at each site, and bed material and benthic macroinvertebrates within the quadrat were collected using a D-frame net with a mesh size of 0.5 mm. The collected bed material was washed, and the recovered organisms were preserved in 70% ethanol.

Specimens were identified and counted to the lowest practicable taxonomic level following Kawai and Tanida [20]. For each study reach, the numbers of individuals collected at the three sites were pooled, and density per square meter (n/m^2) was calculated from the total sampled area of 0.75 m^2. Each individual was assigned to a life type following Takemon [21]. Life type was used as a broad classification reflecting differences in resistance and avoidance strategies to flood disturbance. Among these life types, swimmers and net-spinners were selected for statistical analysis because they differ in mobility and dependence on the bed substrate. Their taxonomic composition and relative abundance are presented in Supplementary Table S1.

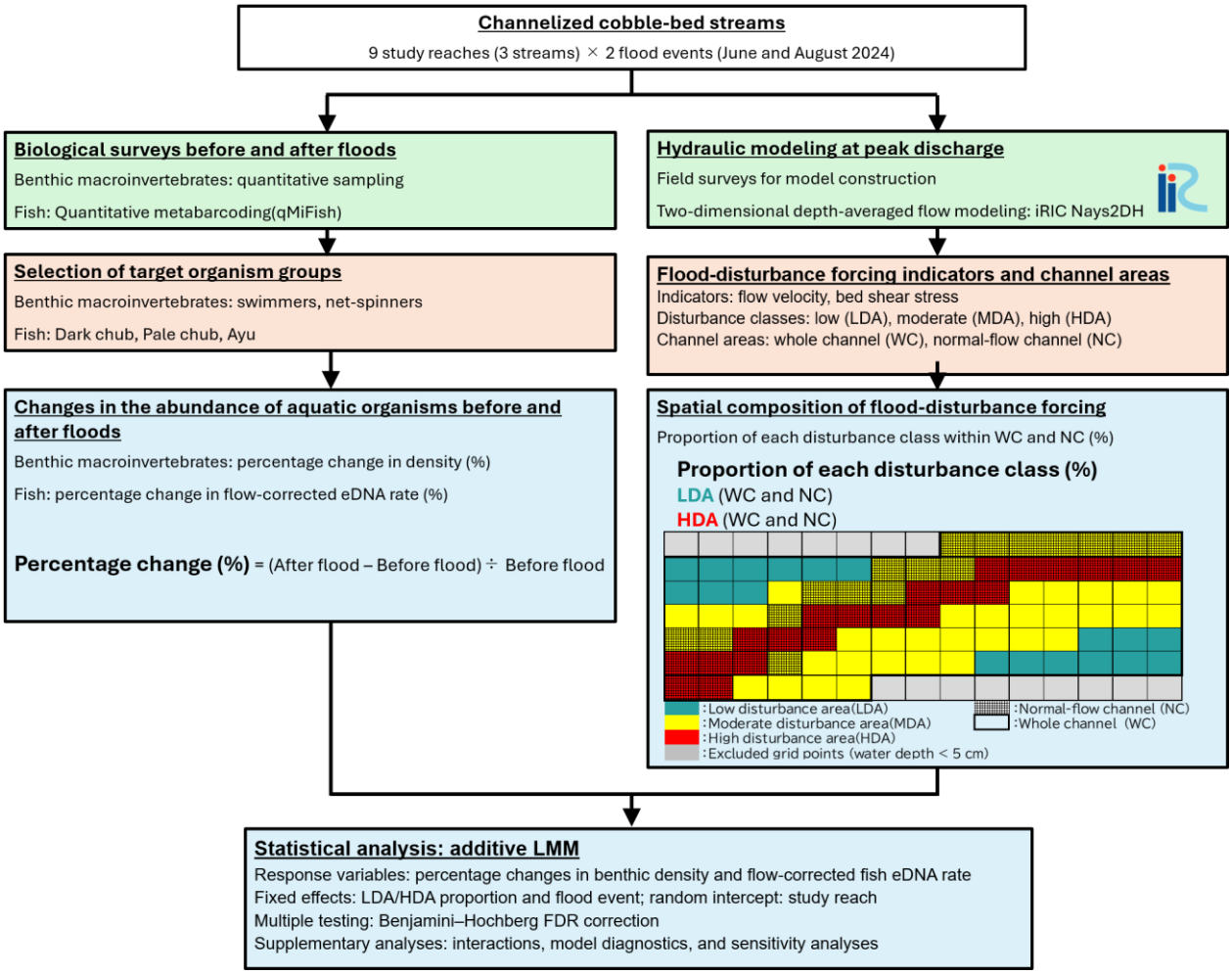


Figure 3. Overall framework of the biological surveys, hydraulic modeling, evaluation of flood-disturbance forcing, and statistical analyses. Flood-disturbance forcing was classified into low-, moderate-, and high-disturbance areas (LDA, MDA, and HDA) within the whole channel (WC) and normal-flow channel (NC).

2.2.2. Fish Survey

For the fish survey, quantitative metabarcoding using qMiFish was conducted to determine species-specific environmental DNA (eDNA) concentrations (copies/L) [22]. Water samples were collected from the center of the low-flow channel at the downstream end of each study reach. One liter of surface water was collected, and 1 mL of 10% benzalkonium chloride solution (OSVAN S, Alinamin Pharmaceutical Co., Ltd., Tokyo, Japan) was added. A cooler blank was used as a negative control during sample transport. Samples were filtered through Whatman GF/F glass-fiber filters (particle retention: 0.7 μm; Cytiva, Tokyo, Japan), and DNA was extracted using a DNeasy Blood & Tissue Kit (QIAGEN GmbH, Hilden, Germany).

The extracted DNA was analyzed by qMiFish using an iSeq 100 Sequencing System (Illumina, Inc., San Diego, CA, USA). Species identification was performed using the MiFish Analytical Pipeline version 2.40 with MiFish DB version 37, with a sequence identity of ≥98.5% with reference sequences in the database used as the primary criterion for taxonomic assignment. Sequences with <98.5% identity were checked using the NCBI web-based Basic Local Alignment Search Tool (BLAST; National Center for Biotechnology Information, Bethesda, MD, USA) [23]. Internal-standard DNA was used for quantitative conversion.

Three fish species were selected for statistical analysis because their eDNA was detected in the study rivers and published information on both cruising and burst swimming speeds was available: Ayu (*Plecoglossus altivelis*), Pale chub (*Opsariichthys platypus*), and Dark chub (*Nipponocypris temminckii*) [24–26] (Figure 3).

2.2.3. Percentage Changes in the Abundance of Aquatic Organisms Before and After Floods

To evaluate changes in the abundance of aquatic organisms before and after the flood events, benthic macroinvertebrate density and the flow-corrected eDNA rate for fish were used. The flow-corrected eDNA rate (copies/s) was calculated by multiplying the eDNA concentration (copies/L) by the discharge at the time of sampling (m^3/s) and a unit conversion factor of 1000 L/m^3, and was used as a proxy for changes in fish abundance [27]. However, the flow-corrected eDNA rate may be influenced by upstream DNA transport, shedding, degradation, and resuspension, and therefore does not directly represent the number of fish within each study reach. Discharge at the time of sampling was estimated using a uniform-flow calculation.

For each response variable, the percentage change from before to immediately after each flood event was calculated as follows:

$$\text{Percentage change (\%)} = \frac{\text{immediate post-flood value} - \text{pre-flood value}}{\text{pre-flood value}} \times 100. \quad (1)$$

The resulting values were defined as the percentage change in density for benthic macroinvertebrates and the percentage change in the flow-corrected eDNA rate for fish. These values were calculated for each target group and study reach for both the June and August flood events. Data for which the pre-flood value was zero, and for which the percentage change could therefore not be calculated, were excluded from the statistical analyses. Percentage changes are bounded below by −100% but have no upper bound. The original pre- and post-flood values used to calculate the percentage changes are provided in Supplementary Table S2.

2.3. Evaluation of the Spatial Composition of Flood-Disturbance Forcing

The workflow for evaluating flood-disturbance forcing is shown on the right side of Figure 3. In this study, flow velocity and bed shear stress acting on aquatic organisms during floods were treated as flood-disturbance forcing. Hydraulic modeling results at peak discharge were classified according to the target organisms, and the proportion of each disturbance class was calculated within the whole channel and normal-flow channel.

2.3.1. Two-Dimensional Depth-Averaged Flow Modeling

Two-dimensional depth-averaged flow modeling was performed using the Nays2DH solver in iRIC version 4.2.1.6985 to evaluate hydraulic conditions during floods [28]. Topographic, land-cover, and bed-material data were obtained before the June 2024 flood event, whereas water levels were monitored during the target flood events.

The main conditions used for the two-dimensional depth-averaged flow modeling in each study reach are summarized in Table 2. For the topographic survey, buffer reaches extending approximately 1–2 channel widths upstream and downstream of each study reach were established, and elevation data were obtained using GNSS surveying with the OPTiM Geo Point application (OPTiM Corporation, Tokyo, Japan). Survey points were generally spaced at approximately 5 m intervals in the longitudinal direction and 2 m intervals in the transverse direction, with additional points surveyed in areas of pronounced topographic variation. The resulting data were interpolated using a triangulated irregular network (TIN) to construct the channel topography model. Land cover was

classified into the normal-flow channel, bare ground, short herbaceous vegetation, tall herbaceous vegetation, woody vegetation, and bamboo stands. Bed material was also collected within the normal-flow channel of each study reach, and d_{16}, d_{50}, and d_{60} were calculated from the cumulative grain-size distribution curve.

Table 2. Main conditions for two-dimensional depth-averaged flow modeling in the nine study reaches.

Item		Study Reach								
		Kawa -ura1	**Kawa -ura2**	**Kawa -ura3**	**Naka -noho1**	**Naka -noho2**	**Naka -noho3**	**Mugi -kura1**	**Mugi -kura2**	**Mugi -kura3**
Topographic data		Topographic survey results obtained in mid-June 2024 (reflecting the topography before the June flood)								
Length (m)		277	171	195	134	146	144	165	134	155
Number of grid cells		184 × 60	100 × 16	121 × 16	89 × 20	121 × 20	120 × 32	150 × 28	149 × 44	259 × 32
Grid size (m)		1.5 × 1.5	1.7 × 1.7	1.6 × 1.6	1.5 × 1.5	1.2 × 1.2	1.2 × 1.2	1.1 × 1.1	0.9 × 0.9	0.6 × 0.6
Grain sizes d_{16}, d_{50} (m)		0.04, 0.07	0.03, 0.06	0.04, 0.06	0.02, 0.05	0.02, 0.08	0.03, 0.08	0.01, 0.04	0.03, 0.05	0.02, 0.05
Roughness coefficient		0.033	0.030	0.030	0.020	0.035	0.028	0.022	0.019	0.034
Roughness coefficient (short herbaceous vegetation)		0.035	None	None	0.025 0.035	None	0.035	0.028	0.025 0.031	0.031 0.035
Vegetation density (m^{-1})		0.750 (MS)	None	None	0.139	0.111 (BL)	0.139 (BL) 0.500 (MS)	0.400 (MS)	0.155 (BL) 0.342 (BS)	0.055 (BL)
Downstream boundary water level		Observed	Calculation	Calculation	Observed	Observed	Observed	Observed	Observed	Observed
Upstream discharge (m^3/s)	Jun.	61	56	47	32	21	18	16	9	6
	Aug.	60	50	41	24	19	14	16	9	6

Note: Jun. and Aug. denote the June and August 2024 flood events, respectively; MS, *Miscanthus sacchariflorus*; BL, broad-leaved trees; BS, bamboo stands. "Calculation" and "Observed" denote uniform-flow-calculated and observed downstream water levels, respectively.

A painted-gravel tracer survey was used to determine bed roughness. In each study reach, 50 gravel particles approximately corresponding to d_{60} were placed within the normal-flow channel, and the number of displaced tracers was recorded before and after the June and August flood events to calculate the proportion of displaced painted-gravel tracers [29,30]. Automatic water-level loggers (HOBO U20L Water Level Logger, Onset Computer Corporation, Bourne, MA, USA; and S&DL mini, OYO Corporation, Tokyo, Japan) were also installed, in principle, at the downstream end of each computational reach to record water levels during the target flood events. Because the water-level loggers at Kawaura 2 and Kawaura 3 were washed away, observations from nearby flood-management water-level gauges were used.

The June and August flood events were simulated for all nine study reaches, with the peak discharge of each event used as the representative flow condition. This approach did not account for temporal variations in hydraulic forcing over the flood hydrograph, including flood duration and the rising and falling limbs. The computational domain included each study reach and the upstream and downstream buffer reaches, resulting in total computational lengths of 134–277 m. The computational grid was designed to represent the boundary between the normal-flow channel and terrestrial areas, channel margins, and lateral channel areas inundated during floods, with grid sizes ranging from

approximately 0.6 × 0.6 to 1.7 × 1.7 m. Grid spacing was approximately uniform within each reach. The channel topography model constructed from measurements obtained before the June flood event was used for both the June and August flood simulations. To clarify the uncertainty associated with using the same topography for both events, we considered the painted-gravel tracer results and visual observations of channel conditions. Across the nine study reaches, the proportions of displaced painted-gravel tracers were 24–48% during the June flood event and 20–46% during the August flood event (Supplementary Table S10). Thus, more than half of the tracers were not displaced in any study reach during either event. Visual inspection during the post-flood survey on 6 September 2024 revealed no substantial apparent changes, compared with the conditions observed before the June flood, in the locations of riffles, runs, and pools, the extent of the normal-flow channel, the surface bed-material composition, or the distribution of herbaceous and woody vegetation. However, tracer displacement does not directly quantify changes in channel topography, and the visual inspection was qualitative and conducted after the August flood. Therefore, changes in bed topography and grain-size distribution could not be ruled out, leaving uncertainty in the estimated flow velocity and bed shear stress for the August flood.

The peak discharge specified at the upstream boundary was generally estimated using a uniform-flow calculation based on the observed water level at the downstream end of each computational reach. The Manning roughness coefficient, n, used for this discharge estimation was determined from the representative grain size, d_{60}, using the Manning–Strickler equation:

$$n = 0.0417 d_{60}^{1/6}, \quad (2)$$

where d_{60} is the representative grain size expressed in meters.

This roughness coefficient was specified separately from the bed roughness coefficient used in the Nays2DH flow calculations. For Kawaura 2 and Kawaura 3, peak discharge was estimated from observations at nearby flood-management water-level gauges. In Nays2DH, the peak discharge of each flood event was specified as the upstream boundary condition, while the observed water level was generally specified as the downstream boundary condition. For Kawaura 2 and Kawaura 3, uniform-flow water levels corresponding to the respective peak discharges were used as the downstream boundary conditions.

The Manning roughness coefficient for the channel bed in Nays2DH was determined separately for each study reach through preliminary calculations using the proportion of displaced painted-gravel tracers. Simulations were performed for multiple roughness coefficients using the peak discharges of both flood events, and the value that minimized the squared error between the proportion of grid points within the normal-flow channel at which the dimensionless bed shear stress for d_{60} was ≥0.05 and the proportion of displaced painted-gravel tracers was adopted [31]. The resulting bed roughness coefficients ranged from 0.019 to 0.035 (Table 2). Flow resistance in vegetated areas was specified based on vegetation height, trunk or stem diameter, and abundance [32,33].

These calculations provided the spatial distributions of depth, depth-averaged velocity, and bed shear stress at the peak discharge of each flood event.

2.3.2. Flood-Disturbance Forcing Indicators and Disturbance Classes

Based on the characteristics of the target organism groups, flow velocity was used as the flood-disturbance forcing indicator for fish, whereas bed shear stress was used for benthic macroinvertebrates (Figure 3). For fish, focusing on the relationship between flow velocity during floods and swimming ability, velocity at 80% water depth was calculated from the depth-averaged velocity. Based on the logarithmic velocity distribution for

rough-wall turbulent flow [34], the relationship between depth-averaged velocity U and velocity $u(y)$ at height y above the bed was expressed as:

$$u(y) = U + u_* \left[2.5 + 5.75 \log_{10} \left(\frac{y}{h}\right)\right], \quad (3)$$

where h is water depth and u_* is friction velocity.

Friction velocity was calculated as:

$$u_* = \sqrt{\frac{\tau}{\rho}}, \quad (4)$$

where τ is bed shear stress and ρ is water density (1000 kg/m^3). Velocity at 80% water depth was defined as the velocity at a point 80% of the water depth below the water surface, corresponding to y/h = 0.2.

Based on the relationship between velocity at 80% water depth and the cruising and burst swimming speeds of each fish species, each grid point was classified as a low-disturbance area (LDA), moderate-disturbance area (MDA), or high-disturbance area (HDA) (Table 3). Grid points with velocities below cruising speed were classified as LDA, those with velocities at or above cruising speed but below burst speed as MDA, and those with velocities at or above burst speed as HDA. Swimming speeds for the three fish species were standardized to a body length of 9 cm [24–26].

Table 3. Criteria used to classify flood-disturbance forcing into low-, moderate-, and high-disturbance areas for the target organisms.

Target Organism	Indicator	Lower Threshold	Upper Threshold	LDA	MDA	HDA
Ayu	Velocity at 80% water depth	Cruising speed: 1.10 m/s	Burst speed: 3.27 m/s	V < 1.10 m/s	1.10 ≤ V < 3.27 m/s	V ≥ 3.27 m/s
Pale chub	Velocity at 80% water depth	Cruising speed: 0.65 m/s	Burst speed: 2.58 m/s	V < 0.65 m/s	0.65 ≤ V < 2.58 m/s	V ≥ 2.58 m/s
Dark chub	Velocity at 80% water depth	Cruising speed: 0.55 m/s	Burst speed: 2.68 m/s	V < 0.55 m/s	0.55 ≤ V < 2.68 m/s	V ≥ 2.68 m/s
Benthic macro invertebrates	Dimensionless bed shear stress	Incipient motion of d_{16}	Incipient motion of d_{50}	$\tau^*(d_{16}) < 0.05$	$\tau^*(d_{16}) \geq 0.05$ and $\tau^*(d_{50}) < 0.05$	$\tau^*(d_{50}) \geq 0.05$

Note: LDA, low-disturbance area; MDA, moderate-disturbance area; HDA, high-disturbance area; V, velocity at 80% water depth; τ*, dimensionless bed shear stress. d_{16} and d_{50} denote the grain sizes for which 16% and 50% of the bed material are finer by weight, respectively.

For benthic macroinvertebrates, dimensionless bed shear stress, τ*, was used as an indicator of the potential for bed-material movement. It was calculated from the bed shear stress τ obtained from the two-dimensional depth-averaged flow modeling as:

$$\tau^* = \frac{\tau}{(\rho_s - \rho) g d}, \quad (5)$$

where $\rho_s - \rho$ is the density difference between the bed material and water (1650 kg/m^3), g is gravitational acceleration (9.81 m/s^2), and d is the target grain size (m).

The d_{16} and d_{50} fractions were used to represent the incipient motion of relatively fine bed material and representative bed material, respectively. Dimensionless bed shear stress was calculated for d_{16} and d_{50} in each study reach, and a critical dimensionless bed shear stress of 0.05 was used as the threshold [31]. Grid points at which $\tau^*(d_{16})$ was below

the critical value were classified as LDA; those at which $\tau^*(d_{16})$ was at or above the critical value but $\tau^*(d_{50})$ remained below the critical value were classified as MDA; and those at which $\tau^*(d_{50})$ was at or above the critical value were classified as HDA (Table 3).

Flood-disturbance forcing was evaluated within the whole channel (WC), representing the channel area inundated during floods, and the normal-flow channel (NC) (Figure 3). For the primary analyses, WC was used for fish and swimmer-type benthic macroinvertebrates to account for their potential movement during floods, whereas NC was used for net-spinners because of their dependence on the bed substrate [5,8,35].

2.3.3. Spatial Composition of Flood-Disturbance Forcing

The spatial composition of flood-disturbance forcing was evaluated as the proportion of each disturbance class within WC and NC (Figure 3). To exclude grid points with very shallow calculated depths near numerical wet–dry boundaries, a minimum depth threshold of 5 cm was applied to the aggregation.

For WC, grid points within each study reach with calculated depths ≥5 cm during each flood event were included. For NC, grid points classified as part of the normal-flow channel in the land-cover survey were included when their calculated depth during the corresponding flood event was ≥5 cm.

For both WC and NC, the numbers of grid points classified as LDA, MDA, and HDA based on flow velocity or bed shear stress were counted, and the proportion (%) of each class relative to the total number of included grid points was calculated. These proportions were used as indicators of the spatial composition of flood-disturbance forcing for each study reach and flood event.

2.4. Statistical Analysis

The statistical analyses were organized into three components (Figure 3). First, primary and supplementary additive linear mixed-effects models (LMMs) were used to examine the relationships between the proportions of disturbance areas and changes in biological indicators before and after floods. Second, additional interaction LMMs were used to examine whether these relationships differed between the two flood events. Third, model diagnostics and sensitivity analyses were conducted to identify limitations in model fitting and assess the sensitivity of the estimated relationships to data selection, estimation methods, and disturbance-class thresholds.

2.4.1. Primary and Supplementary Additive LMMs

The response variables were the percentage changes in the flow-corrected eDNA rates of three fish species (Ayu, Pale chub, and Dark chub) and the densities of two benthic macroinvertebrate life types (swimmers and net-spinners).

Based on the ecological characteristics of the target organisms, 10 additive linear mixed-effects models (LMMs) were designated as the primary analyses (Figure 3). For the three fish species, six models used velocity-based LDA or HDA proportions within the whole channel (WC). For swimmers, two models used bed-shear-stress-based LDA or HDA proportions within WC, whereas for net-spinners, two models used the corresponding proportions within the normal-flow channel (NC). An additional 22 models examining alternative combinations of forcing indicators and channel areas were designated as supplementary analyses, resulting in 32 additive LMMs in total.

Each LMM included one disturbance-area proportion (either LDA or HDA) and flood event as fixed effects, with study reach as a random intercept to account for repeated observations within reaches. Flood event was treated as a categorical variable with two levels (June and August). Each study reach × flood-event combination was treated as an observational unit, and the two flood events were shared across the three study rivers.

Although MDA proportions were calculated to characterize the spatial composition of forcing, they were not included in the LMMs.

To account for multiple testing, *p*-values for the LDA or HDA coefficients were adjusted using the Benjamini–Hochberg (BH) procedure separately for the 10 primary and 22 supplementary models. A BH-adjusted *p*-value below 0.05 was considered statistically significant. The LMMs were fitted by restricted maximum likelihood, and *p*-values and unadjusted 95% confidence intervals for the coefficients were calculated using Satterthwaite degrees of freedom.

In addition, Pearson's product–moment correlation coefficients were calculated between LDA and HDA proportions separately for WC and NC for each velocity- and bed-shear-stress-based indicator.

2.4.2. Flood-Event Interaction Analysis

To examine whether the estimated relationships differed between the June and August flood events, additional LMMs including an interaction between the LDA or HDA proportion and flood event were fitted for all 32 model combinations. These analyses examined whether the slopes of the relationships differed between the two flood events. The interaction *p*-values were adjusted using the BH procedure separately for the 10 primary and 22 supplementary combinations. The interaction analyses were supplementary and were not used to select the primary additive LMMs.

2.4.3. Model Diagnostics

Model diagnostics were conducted to identify potential limitations in the assumptions and estimation of the additive LMMs. Residual distributions and residual variation were examined to assess the adequacy of the fitted models. Singular fits were also checked to identify models in which the random-effect structure could not be fully estimated from the available data.

2.4.4. Robustness of Regression Coefficients

Sensitivity analyses were conducted for the 10 primary additive LMMs to examine whether the estimated regression coefficients depended strongly on particular rivers, observations, or estimation methods.

First, river was additionally included as a fixed effect to assess the influence of differences among rivers. Second, models were refitted after excluding individual observations, study reaches, or rivers to examine whether the estimated coefficients were strongly influenced by particular data. Third, robust LMMs were fitted to assess sensitivity to the estimation method. The direction and magnitude of the LDA or HDA coefficients were compared across these analyses.

2.4.5. Sensitivity to Disturbance-Class Thresholds

Because the proportions of LDA and HDA depend on the thresholds used to classify flood-disturbance forcing, additional sensitivity analyses were conducted to examine the influence of these threshold settings.

For fish, the swimming-speed thresholds were varied by ±10% and ±20%. For benthic macroinvertebrates, the critical dimensionless bed shear stress threshold was varied from 0.04 to 0.06. The modeled hydraulic conditions were kept unchanged, and the proportions of LDA and HDA were recalculated under each threshold setting. The corresponding LMM coefficients were then examined to assess how the estimated relationships depended on the disturbance-class thresholds.

All statistical analyses were performed using R version 4.3.3 (R Foundation for Statistical Computing, Vienna, Austria) [36], with the lme4 (version 1.1-35.1) and lmerTest (version 3.1-3) packages.

2.5. Use of Generative AI in Manuscript Preparation

During manuscript preparation and revision, ChatGPT (GPT-6; OpenAI) was used to assist with English translation, language editing, manuscript organization, development of R code for statistical analyses, and preparation of figures and tables. Statistical analyses supported by AI-assisted R code were also performed in the authors' own R environment. All AI-assisted outputs, including statistical results, figures, and tables, were reviewed and verified by the authors.

3. Results

3.1. Changes in the Abundance of Aquatic Organisms Before and After Floods

Table 4 shows the percentage changes in benthic macroinvertebrate density before and after the flood events. For swimmers, density decreased in many reaches during the June flood event, with no individuals detected after the flood in some reaches, whereas decreases, increases, and no change were observed among reaches during the August flood event. For net-spinners, density decreased in eight of the nine study reaches during both the June and August flood events. Across the four surveys, *Isonychia japonica* accounted for 95.6% of the summed swimmer density, whereas *Hydropsyche orientalis* and *Stenopsyche sauteri* accounted for 63.7% and 25.8% of the summed net-spinner density, respectively (Supplementary Table S1).

Table 4. Percentage changes in benthic macroinvertebrate density before and after the June and August flood events.

Life Types	Percentage Change in Benthic Macroinvertebrate Density (%)								
	Kawaura1	**Kawaura2**	**Kawaura3**	**Nakanoho1**	**Nakanoho2**	**Nakanoho3**	**Mugikura1**	**Mugikura2**	**Mugikura3**
Swimmers	−100	−67	−78	−100	−100	0	300	−82	−89
	−100	−92	0	380	−74	200	100	−50	0
Net-Spinners	−77	−36	−50	−80	−70	−93	−26	−22	267
	−94	−88	−76	−57	−80	−25	−14	86	−75

Note: Upper and lower rows indicate the June and August flood events, respectively.

Table 5 shows the percentage changes in the flow-corrected eDNA rates of Ayu, Pale chub, and Dark chub before and after the flood events. For Ayu, decreases occurred in many reaches during the June flood event, whereas increases were more common during the August flood event. For Pale chub, decreases were also more common during the June flood event, whereas increases occurred in three of the six reaches included in the analysis during the August flood event. For Dark chub, increases were observed during both flood events, particularly during the August flood event, when increases occurred in eight of the nine reaches. At Kawaura 1, Dark chub showed greater increases than at the other reaches during both flood events.

Table 5. Percentage changes in the flow-corrected eDNA rate of fish before and after the June and August flood events.

Species	Percentage Change in Flow-Corrected eDNA Rate (%)								
	Kawaura1	**Kawaura2**	**Kawaura3**	**Nakanoho1**	**Nakanoho2**	**Nakanoho3**	**Mugikura1**	**Mugikura2**	**Mugikura3**
Dark chub	1046	−46	36	−23	−33	453	−41	39	−20
	1278	6	11	123	−28	187	1	415	108

Pale chub	111	−8	−1	−73	-	-	−46	−53	-
	25	−40	−29	−69	-	-	178	164	-
Ayu	142	−6	−41	-	-	−100	−83	−58	−67
	19	−51	1	245	−100	-	16	229	333

Note: Upper and lower rows indicate the June and August flood events, respectively. A hyphen (-) indicates that the percentage change could not be calculated.

3.2. Spatial Composition of Flood-Disturbance Forcing

3.2.1. Spatial Distribution of Flood-Disturbance Forcing

As an example of the spatial distribution of flood-disturbance forcing, Figure 4 shows the evaluation results for the June flood event in the three Kawaura River reaches. LDA, MDA, and HDA coexisted within the channel, and their distributions differed between channel-margin and central-channel areas and between the normal-flow channel and lateral channel areas inundated during floods. In the bed-shear-stress-based evaluation, some reaches had HDA distributed in the central part of the channel and LDA along the channel margins. Even within the same study reach, the spatial distributions of the disturbance classes differed between the velocity- and bed-shear-stress-based evaluations. For example, at Kawaura 1, bed-shear-stress-based LDA was more widely distributed than Dark chub velocity-based LDA. In contrast, at Kawaura 2, Dark chub velocity-based HDA was nearly absent, whereas bed-shear-stress-based HDA was widely distributed within the channel. The spatial distributions of flood-disturbance forcing for all nine study reaches during both flood events are shown in Supplementary Figure S1.

3.2.2. Proportions of LDA and HDA

Table 6 shows the proportions of LDA and HDA across the nine study reaches. For the bed-shear-stress-based indicator within WC, the proportions of LDA and HDA differed among study reaches. For example, during the June flood event, the proportion of LDA was high at Kawaura 1, whereas the proportion of HDA was high at Kawaura 2, indicating differences in the spatial composition of flood-disturbance forcing even within the same river. For the fish velocity indicators, the proportions of LDA and HDA also differed among target species and study reaches.

Table 6. Proportions of low-disturbance areas (LDA) and high-disturbance areas (HDA) for the forcing indicators and channel areas used in the primary analyses.

Target/Indicator	Class	Values Represent the Proportion of Each Disturbance Class (%)								
		Kawa-ura1	**Kawa-ura2**	**Kawa-ura3**	**Naka-noho1**	**Naka-noho2**	**Naka-noho3**	**Mugi-kura1**	**Mugi-kura2**	**Mugi-kura3**
Dark chub, velocity (WC)	LDA	33	5.7	13.1	5.8	8.7	33.8	31.2	28.9	12.4
		31.9	5.4	11.5	4.1	9.1	31.1	31.3	29.2	12.6
	HDA	0.7	0	11.9	65.5	0	23.2	18.5	21.5	0
		0.5	0	2.1	53.5	0	16.9	18.7	25	0
Pale chub, velocity (WC)	LDA	43.9	6.5	16.5	6.1	12.6	37.6	34.1	31.5	14.8
		44.2	6.8	15.3	4.9	12.4	34.1	34.5	30.9	14.8
	HDA	3.2	2.5	25.2	66.7	0	25.5	24.9	24.6	0
		2.7	0	6.8	57.2	0	21.1	24	27.1	0
Ayu, velocity (WC)	LDA	66.1	17.8	25.9	9.5	24.5	46.1	43.6	43.5	30.3
		66.3	19.2	25.9	13.5	25.5	44.4	43.5	43.4	30.8
	HDA	0	0	0	43.9	0	3.6	1.5	8.2	0
		0	0	0	24.4	0	1.1	1.3	10.1	0
	LDA	75.7	21	31.5	24.7	20.8	43.9	42.4	56.8	16.9
		75.1	21.2	31.8	24.5	20	45.7	42.3	55.5	17.1

Swimmers, bed shear stress (WC)	HDA	16.4	57.7	53.3	64.5	38.8	29.5	36.2	27.4	16
		16.2	48.1	50.5	56	31.1	27.1	36.5	29.2	15.1
Net-spinners, bed shear stress (NC)	LDA	38.2	13.9	17.9	17.2	13.6	34.1	27.3	63.2	11.4
		36.9	14.4	19.1	19.3	13	36.8	27.8	61.3	11.6
	HDA	43.1	69.4	64.3	66.3	42.7	37.5	47.1	20.8	17.1
		42.5	58.6	60	56.7	34	33.6	47.5	22	16.2

Note: Upper and lower rows indicate the June and August flood events, respectively. LDA, low-disturbance area; HDA, high-disturbance area; WC, whole channel; NC, normal-flow channel.

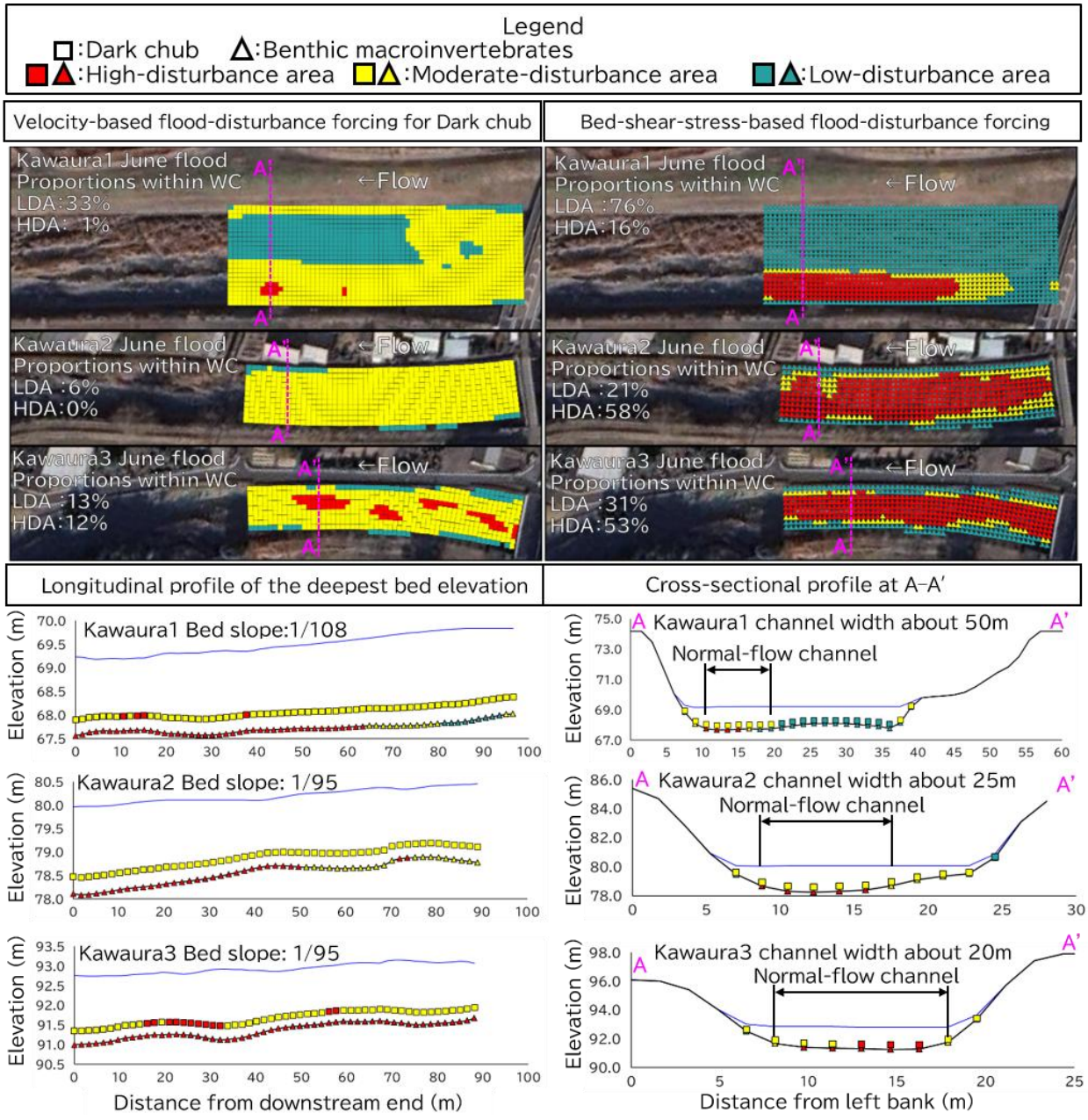


Figure 4. Examples of the spatial distribution of flood-disturbance forcing during the June 2024 flood event in the three Kawaura River study reaches. Disturbance classes were defined using flow velocity or bed shear stress. The upper panels show plan-view distributions of the disturbance classes based on Dark chub velocity (**left**) and bed shear stress for benthic macroinvertebrates (**right**), whereas the lower panels show longitudinal profiles of the deepest bed elevation (**left**) and cross-sectional profiles at A–A′ (**right**) for each study reach.

Comparison between flood events showed that the proportion of bed-shear-stress-based LDA within WC was generally similar between the two events in many reaches, whereas the proportion of HDA differed between flood events in some reaches. For the fish velocity indicators, differences in LDA proportions between flood events were generally small, whereas HDA proportions varied among fish species and study reaches.

Comparison between WC and NC showed that, for the bed shear stress indicator, the proportion of LDA was smaller in NC than in WC in 16 of the 18 cases, whereas the proportion of HDA was greater in NC. Similarly, for the velocity indicators of all three fish species, the proportion of LDA was smaller in NC than in WC in 16 of the 18 cases for each species. In contrast, differences in HDA proportions between WC and NC varied among fish species, and HDA was absent in many cases for Ayu.

Supplementary Table S3 shows the results of the correlation analyses between the proportions of LDA and HDA. The absolute values of the correlation coefficients were below 0.5 for all combinations. For the bed shear stress indicator, negative correlation coefficients were observed in both WC and NC, with an unadjusted *p*-value of 0.0489 in WC ($r = -0.470$). For the velocity indicators of Pale chub and Dark chub, the absolute values of the correlation coefficients were small in both WC and NC. The sensitivity of LDA and HDA proportions to the threshold settings is summarized in Supplementary Table S4.

3.3. Relationships Between the Spatial Composition of Flood-Disturbance Forcing and Changes in the Abundance of Aquatic Organisms

3.3.1. Primary and Supplementary Additive LMMs

The results of the 10 primary additive LMMs are presented in Table 7, and those of all 32 additive LMMs, including the 22 supplementary models, are provided in Supplementary Table S5.

Table 7. Results of the primary additive linear mixed-effects models relating the spatial composition of flood-disturbance forcing to changes in the abundance of aquatic organisms before and after floods.

Target Organism/Life Type	Indicator	Channel Area	Class	n	Additive LMM			
					β	95% CI	*p*-Value	BH-Adjusted *p*-Value
Dark chub	Velocity	WC	LDA	18	20.58	−1.65 to 42.82	0.065	0.217
Dark chub	Velocity	WC	HDA	18	1.76	−11.95 to 15.47	0.785	0.872
Pale chub	Velocity	WC	LDA	12	3.48	0.16 to 6.80	0.042	0.210
Pale chub	Velocity	WC	HDA	12	−1.02	−3.92 to 1.87	0.445	0.872
Ayu	Velocity	WC	LDA	15	0.71	−4.19 to 5.62	0.757	0.872
Ayu	Velocity	WC	HDA	15	7.83	−3.13 to 18.79	0.145	0.363
Swimmers	Bed shear stress	WC	LDA	18	−0.35	−5.48 to 4.79	0.878	0.878
Swimmers	Bed shear stress	WC	HDA	18	1.55	−4.32 to 7.43	0.555	0.872
Net-spinners	Bed shear stress	NC	LDA	18	0.48	−2.45 to 3.41	0.731	0.872
Net-spinners	Bed shear stress	NC	HDA	18	−2.55	−4.94 to −0.16	0.038	0.210

Note: The additive linear mixed-effects models included the proportion of LDA or HDA and flood event as fixed effects, with study reach as a random intercept. β represents the estimated change in

the response variable (percentage points) per 1-percentage-point increase in the proportion of LDA or HDA, adjusted for flood event. CI, 95% confidence interval; *p*-value, unadjusted *p*-value for β; BH-adjusted *p*-value, *p*-value adjusted for multiple testing across the 10 primary models using the Benjamini–Hochberg procedure. LDA, low-disturbance area; HDA, high-disturbance area; WC, whole channel; NC, normal-flow channel.

In the primary analyses for fish, positive coefficients were estimated for the relationships between the proportion of velocity-based LDA within WC and the percentage changes in the flow-corrected eDNA rates of Dark chub (β = 20.58, $p = 0.065$) and Pale chub (β = 3.48, $p = 0.042$). For Ayu, neither the LDA nor the HDA model within WC showed an unadjusted *p*-value below 0.05. Figure 5 shows the observations and additive LMM predictions for the primary fish models.

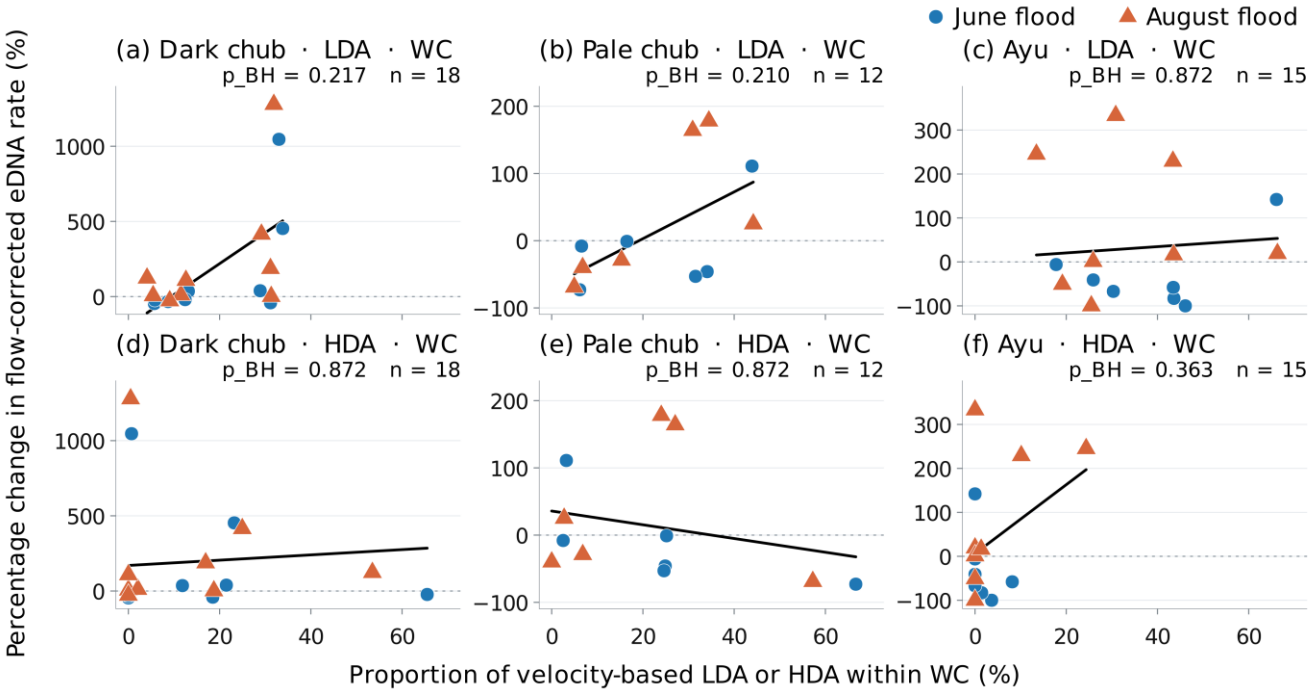


Figure 5. Relationships between the spatial composition of flood-disturbance forcing and percentage changes in the flow-corrected eDNA rate of fish in the primary analyses. Velocity-based low-disturbance areas (LDA) and high-disturbance areas (HDA) within the whole channel (WC) are shown for Dark chub, Pale chub, and Ayu. Points represent study reach × flood-event observations for the June and August 2024 flood events. Black lines represent fixed-effect predictions from additive linear mixed-effects models, averaged across the observed frequencies of the two flood events, with study-reach random intercepts set to zero. BH-adjusted *p*-values (p_BH) refer to the indicator coefficients adjusted across the 10 primary models using the Benjamini–Hochberg procedure.

For benthic macroinvertebrates, a negative coefficient was estimated for the relationship between the proportion of bed-shear-stress-based HDA within NC and the percentage change in net-spinner density (β = −2.55, $p = 0.038$). Neither the LDA model for net-spinners nor the LDA and HDA models for swimmers showed unadjusted *p*-values below 0.05. Figure 6 shows the observations and additive LMM predictions for the primary benthic macroinvertebrate models.

Thus, among the 10 primary models, unadjusted *p*-values were below 0.05 for Pale chub with velocity-based LDA within WC and net-spinners with bed-shear-stress-based HDA within NC. However, after BH correction across the 10 primary models, the adjusted

p-values for both coefficients were 0.210, and no LDA or HDA coefficient remained statistically significant.

Among the 22 supplementary additive LMMs, the smallest unadjusted *p*-value was obtained for Dark chub with bed-shear-stress-based LDA within WC ($\beta = 16.09$, $p = 0.0046$). However, this coefficient was not statistically significant after BH correction across the 22 supplementary models (BH-adjusted $p = 0.102$), and no supplementary model showed a statistically significant LDA or HDA coefficient after correction (Supplementary Table S5).

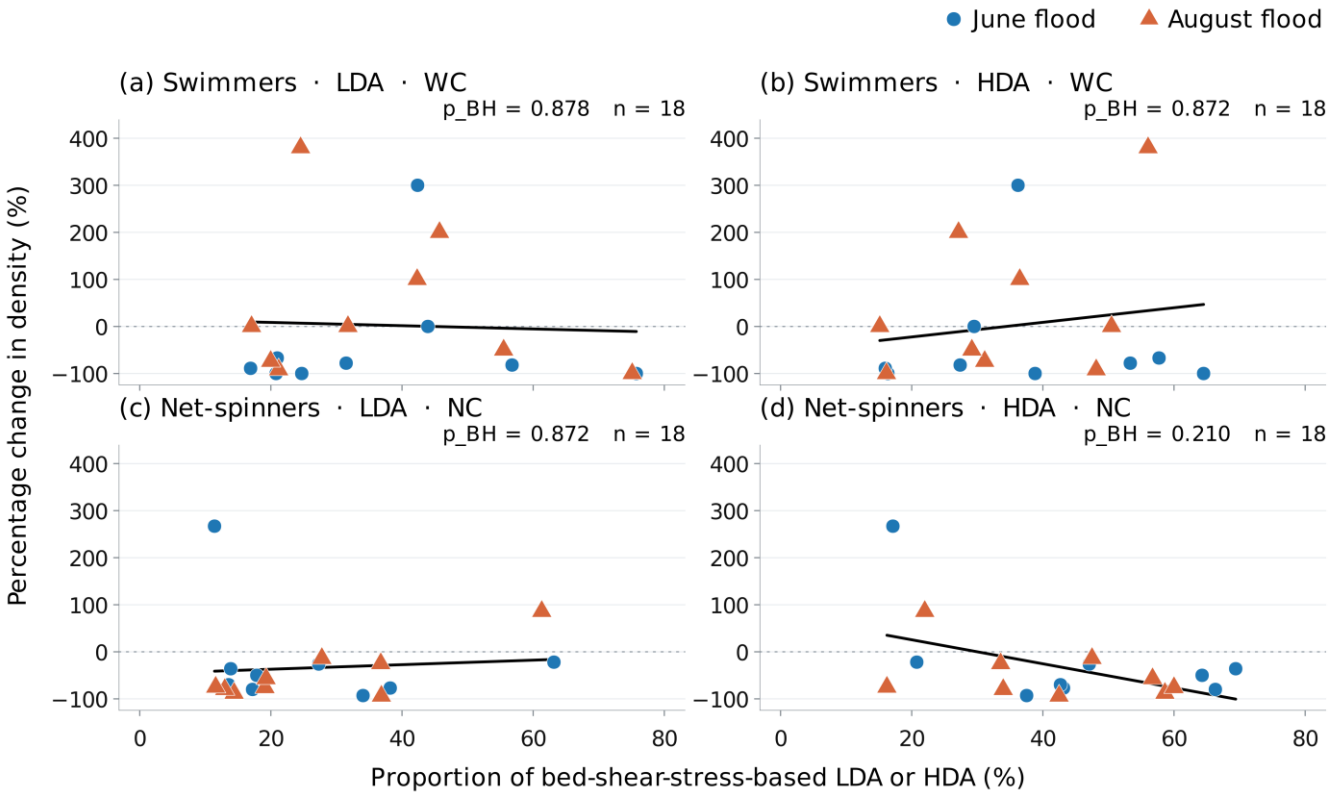


Figure 6. Relationships between the spatial composition of flood-disturbance forcing and percentage changes in benthic macroinvertebrate density in the primary analyses. Bed-shear-stress-based low-disturbance areas (LDA) and high-disturbance areas (HDA) were evaluated within the whole channel (WC) for swimmers and the normal-flow channel (NC) for net-spinners. Points represent study reach × flood-event observations for the June and August 2024 flood events. Black lines represent fixed-effect predictions from additive linear mixed-effects models, averaged across the observed frequencies of the two flood events, with study-reach random intercepts set to zero. BH-adjusted *p*-values (p_BH) refer to the indicator coefficients adjusted across the 10 primary models using the Benjamini–Hochberg procedure.

3.3.2. Flood-Event Interaction Analysis

The additional interaction LMMs showed no statistically significant interactions between the proportion of LDA or HDA and flood event after BH correction (Supplementary Table S6). In the supplementary model for Pale chub using velocity-based LDA within NC, the interaction had an unadjusted *p*-value of 0.0267, but the BH-adjusted *p*-value was 0.587.

3.3.3. Model Diagnostics and Sensitivity Analyses

Model diagnostics identified singular fits in six of the 10 primary additive LMMs, including both models for Pale chub, Ayu, and net-spinners. Residual normality tests indicated departures from normality in all four benthic macroinvertebrate models, with

Shapiro–Wilk *p*-values below 0.05. In contrast, none of the six fish models showed a statistically significant departure from residual normality (p = 0.0506–0.4061) (Supplementary Table S7).

Sensitivity analyses of the regression coefficients showed differences in the stability of the estimates among models. For Dark chub, the positive coefficient for velocity-based LDA within WC (β = 20.58) remained positive under all data-exclusion conditions, although it ranged from +7.42 to +26.37 when individual study reaches were excluded and decreased to +12.04 under robust estimation. For Pale chub, the corresponding positive coefficient (β = 3.48) was also retained under all data-exclusion conditions, ranging from +2.92 to +4.91 when individual rivers were excluded. In contrast, the negative coefficient for bed-shear-stress-based HDA within NC for net-spinners (β = −2.55) ranged from −3.22 to +0.30 when individual rivers were excluded and decreased in magnitude to −1.03 under robust estimation (Supplementary Table S8).

Sensitivity analyses of disturbance-class thresholds showed that the estimated coefficients varied with threshold settings. For Dark chub, the coefficient for velocity-based LDA within WC ranged from +7.78 to +21.96, compared with +20.58 in the original model. The corresponding coefficient for Pale chub ranged from +3.02 to +4.82, compared with +3.48 in the original model. For net-spinners, the coefficient for bed-shear-stress-based HDA within NC ranged from −2.55 to −1.91, compared with −2.55 in the original model. The signs of these three coefficients were retained across the tested threshold settings. Overall, coefficient signs were retained in nine of the 10 primary models (Supplementary Table S9).

4. Discussion

4.1. Relationships Between Flood-Disturbance Forcing and Changes in the Abundance of Aquatic Organisms

This study examined whether hydraulically estimable indicators of the spatial composition of flood-disturbance forcing were related to changes in the abundance of aquatic organisms before and after floods. In the primary analyses, positive coefficients were estimated for velocity-based LDA within the whole channel (WC) for Dark chub and Pale chub, whereas a negative coefficient was estimated for bed-shear-stress-based HDA within the normal-flow channel (NC) for net-spinners. These results showed different trends in the estimated relationships among organism groups under the combinations of forcing indicators and channel areas selected for each group. However, none of these relationships was statistically significant after BH correction, and no significant relationships were detected in the other primary or supplementary additive LMMs. Consequently, the results did not identify a statistically supported combination of forcing indicator and channel area for any organism group.

For Dark chub and Pale chub, the estimated coefficients for velocity-based LDA within WC were positive, although they were not statistically significant after BH correction. Positive percentage changes in the flow-corrected eDNA rate were observed in some reaches for both species, and the flow-corrected eDNA rate of Dark chub in particular increased in many reaches after the August flood event. Fish have been reported to use low-velocity areas along channel margins and in lateral channel areas during high flows [37,38], and movements beyond individual river reaches can also occur [11]. Thus, in reaches with a greater proportion of low-velocity areas within WC, more space may have been available for both individuals remaining within the reach and those moving during floods to avoid strong flows, potentially contributing to fish persistence or post-flood redistribution. However, refuge use and redistribution were not directly observed in this study. Moreover, the flow-corrected eDNA rate does not directly represent the number of fish within a study reach, and an increase in this rate cannot therefore be interpreted

directly as an increase in fish abundance [27]. In addition, the spatial extent represented by riverine eDNA does not necessarily coincide with the approximately 100 m hydraulic evaluation reach; therefore, caution is required when interpreting the estimated relationships as direct changes in fish abundance within individual study reaches.

For Dark chub, the supplementary analyses yielded positive and negative coefficients for bed-shear-stress-based LDA and HDA within WC, respectively, but neither was statistically significant after BH correction. Thus, these results do not establish whether changes in the flow-corrected eDNA rate were more closely related to flow velocity or bed shear stress. For Pale chub, the interaction between flood event and velocity-based LDA within NC was not statistically significant after BH correction, and a difference in the relationship between flood events could not be established. For Ayu, no clear relationships were detected in either the primary or supplementary analyses, and one possible explanation is movement at spatial scales broader than the approximately 100 m study reaches, although such movement was not directly measured.

For net-spinners, the estimated coefficient for bed-shear-stress-based HDA within NC was negative, although it was not statistically significant after BH correction. Because net-spinners construct nets and retreats on bed material, streambed stability within their normal-flow habitat is likely to be important. Increased bed shear stress and streambed instability have also been reported to induce downstream drift of benthic macroinvertebrates [4]. Furthermore, the supplementary analyses showed no statistically significant relationships after BH correction with bed-shear-stress-based LDA or HDA within WC. The negative coefficient within NC is consistent with a possible influence of strong streambed disturbance on density changes, but does not demonstrate that NC is more ecologically relevant than WC. In addition, net-spinner density was dominated by a small number of taxa (Supplementary Table S1), and the present study could not distinguish losses through drift or mortality from subsequent recolonization.

For swimmers, no significant relationships were detected with bed-shear-stress-based LDA or HDA within either WC or NC after BH correction. For this life type, changes in density may depend not only on the spatial composition of forcing at peak discharge but also on the time available to move into low-forcing areas during rising flows and on post-flood recolonization. Sueyoshi et al. [8] reported that swimmer-type benthic macroinvertebrates used multiple flow refugia during a snowmelt flood and rapidly recovered in the main channel after the flood, and also highlighted the importance of flood duration and rates of discharge increase and decrease. Because the present study evaluated flood-disturbance forcing at peak discharge, such temporal processes were not captured. Furthermore, the swimmer group was strongly dominated by *Isonychia japonica* (Supplementary Table S1), so the observed density changes may not represent a general response across swimmer taxa. These potential explanations could not be distinguished using the present data, and the absence of a statistically significant relationship does not demonstrate that peak-discharge forcing is ecologically unimportant.

Overall, the hypothesized relationships between the spatial composition of flood-disturbance forcing and changes in abundance were not statistically supported after BH correction. Although the directions of some estimated coefficients were consistent with possible ecological mechanisms suggested by previous studies, the analyses did not establish that particular forcing indicators or channel areas were more appropriate for specific organism groups. Differences in the estimated relationships among species or life types were not formally tested. Moreover, the flow-corrected eDNA rate for fish and density for benthic macroinvertebrates represent different biological measurements, limiting direct comparisons between these groups. Thus, while the hydraulically estimable proportions of LDA and HDA provide a means of characterizing the spatial composition of flood-time

forcing, further validation is required to establish their ecological relevance for channel planning and design.

4.2. Spatial Composition of Flood-Disturbance Forcing

In this study, LDA, MDA, and HDA coexisted in several study reaches, indicating that flood-disturbance forcing was spatially heterogeneous. This is consistent with Lancaster and Hildrew [5], who showed that low-forcing areas can persist even under high-flow conditions, and Matthaei et al. [6], who demonstrated spatial heterogeneity in streambed disturbance. These findings indicate the value of characterizing not only reach-averaged flow velocity or bed shear stress but also the spatial composition of areas exposed to different levels of forcing during floods. In the present study, this spatial composition was quantified using the proportions of disturbance classes derived from hydraulic modeling results.

In many cases, NC had a greater proportion of bed-shear-stress-based HDA and a smaller proportion of LDA than WC. For the fish velocity indicators, the proportion of LDA was also smaller in NC than in WC in many cases. Thus, the spatial composition of flood-disturbance forcing itself differed depending on whether lateral channel areas inundated during floods were included in the evaluation. This finding highlights the importance of explicitly defining the channel area used to evaluate flood-disturbance forcing, although the present analyses did not establish which channel area was more appropriate for individual organism groups.

The correlations between the proportions of LDA and HDA were not strong, indicating that a reach with a large proportion of low-disturbance area did not necessarily have a small proportion of high-disturbance area. Different spatial compositions of flood-disturbance forcing were therefore formed among study reaches through the coexistence of LDA, MDA, and HDA in different proportions. However, because the proportions of LDA, MDA, and HDA sum to 100%, these correlations should be interpreted descriptively rather than as evidence that the proportions vary independently.

The proportions of the disturbance classes evaluated in this study represent the extent of each disturbance class within the channel but not the location and connectivity of these areas. These proportions also depend on the thresholds used to define the disturbance classes (Supplementary Table S4). For fish to use low-velocity areas, not only their extent but also accessibility to channel margins and lateral channel areas and connectivity among low-velocity areas may be important. The actual use of these areas by fish was not directly observed in this study. Future evaluation of the location and connectivity of low-disturbance areas, in addition to their proportions, may provide a more direct characterization of the availability of these areas to aquatic organisms during floods.

4.3. Implications for Channel Design and Management in Channelized Streams

For the design and management of channelized streams, the spatial composition of flood-disturbance forcing during floods may provide additional information alongside assessments of normal-flow habitats. Channelization has been reported to influence hydraulic heterogeneity and the formation of flow refugia during floods [7,14], whereas restoring structural heterogeneity does not necessarily result in clear responses by fish or benthic macroinvertebrates [13]. The present study examined combinations of forcing indicators and channel areas selected according to the characteristics of the target organisms. However, the analyses did not establish that any particular combination was more appropriate for a given organism group.

Specifically, positive coefficients were estimated for the proportion of velocity-based LDA within WC in the models for changes in the flow-corrected eDNA rates of Dark chub and Pale chub, whereas a negative coefficient was estimated for the proportion of bed-

shear-stress-based HDA within NC in the model for changes in net-spinner density. None of these coefficients was statistically significant after BH correction. In addition, including lateral channel areas inundated during floods within WC resulted in relatively greater proportions of low-disturbance areas in many cases. As a potential application to channel design, channel forms that create low-forcing spaces along channel margins and in lateral channel areas could be examined when considering flood-time conditions for fish. Inter-levee floodplains and partial channel widening are examples of channel forms that may create such spaces [35,39]. In contrast, for organisms with a strong dependence on bed substrates, such as net-spinners, the extent of strong streambed disturbance within the normal-flow channel may also warrant consideration. However, the potential biological benefits of such channel designs were not evaluated in this study.

Two-dimensional depth-averaged flow modeling allows alternative excavation geometries, channel widths, and cross-sectional designs to be compared in terms of the spatial composition of flood-disturbance forcing as well as flow conveyance capacity. Such evaluation may provide one approach for examining channel geometry while considering the formation of low- and high-disturbance areas during floods according to the target organisms.

This study was based on two flood events across nine reaches in three streams and did not compare conditions before and after channelization or with natural river channels. Although the LMMs accounted for repeated observations within study reaches, the two flood events were shared across the three rivers, and the limited number of independent flood events and rivers constrained the generalizability of the estimated relationships. At each study reach, the two flood events had generally similar peak discharges, so the range of flood magnitude examined within each reach was limited. Furthermore, because no unaffected control reaches were included, changes in abundance between the pre- and post-flood surveys may have been influenced by seasonal processes as well as flood disturbance. Excluding observations with zero pre-flood values may also have introduced selection bias. No coefficient for the LDA or HDA proportions was statistically significant after BH correction, and the asymmetric percentage-change data, singular fits, departures from residual normality, and sensitivity to data exclusions warrant caution when interpreting the estimated relationships (Supplementary Tables S7 and S8). Therefore, the relationships between the spatial composition of flood-disturbance forcing and changes in abundance, as well as the effects of channelization itself, should be examined under a wider range of river and flood conditions in future studies.

5. Conclusions

This study examined the relationships between the spatial composition of flood-disturbance forcing during two flood events and changes in the abundance of aquatic organisms before and after the floods across nine study reaches in three channelized cobble-bed streams. Classification of flood-disturbance forcing into LDA, MDA, and HDA based on flow velocity and bed shear stress showed that areas exposed to different levels of forcing coexisted within the same study reach and that their spatial composition differed among study reaches, flood events, and between the whole channel and normal-flow channel. In the primary analyses, positive coefficients were estimated for the relationships between the percentage changes in the flow-corrected eDNA rates of Dark chub and Pale chub and the proportion of velocity-based LDA within the whole channel, whereas a negative coefficient was estimated for the relationship between the percentage change in net-spinner density and the proportion of bed-shear-stress-based HDA within the normal-flow channel. The unadjusted p-values for the coefficients of Pale chub and net-spinners were below 0.05. However, the coefficients for the proportions of LDA or HDA were not statistically

significant after BH correction in any of the 32 models, comprising 10 primary and 22 supplementary models.

The estimated associations describe the individual combinations of organism groups, forcing indicators, and channel areas examined in this study and should not be interpreted as evidence that biological responses differed among organism groups. Although the ecological relevance of these combinations remains uncertain, the spatial composition of flood-disturbance forcing may provide complementary information for evaluating flood-time conditions alongside normal-flow habitats. Spatial evaluation of flood-disturbance forcing using two-dimensional depth-averaged flow modeling may provide useful information for examining channel width, cross-sectional geometry, and lateral channel areas while considering both flow conveyance capacity and flood-time habitat conditions for aquatic organisms. However, this study did not fully establish the ecological validity of the combinations of forcing indicators and channel areas for individual organism groups. Further studies are needed to clarify the ecological relevance of these hydraulically estimable indicators.

Supplementary Materials: The following supporting information can be downloaded at: https://www.mdpi.com/article/10.3390/w18222863/s1, Figure S1: Spatial distributions of flood-disturbance forcing for the nine study reaches during the June and August 2024 flood events; Table S1: Taxonomic composition, mean density, and relative abundance of swimmer- and net-spinner-type benthic macroinvertebrates before and after the June and August 2024 flood events; Table S2: Pre- and post-flood values of benthic macroinvertebrate density and flow-corrected fish eDNA rate used to calculate percentage changes; Table S3: Results of correlation analyses between the proportions of low-disturbance areas (LDA) and high-disturbance areas (HDA); Table S4: Sensitivity of low-disturbance area (LDA) and high-disturbance area (HDA) proportions to threshold settings; Table S5: Results of all 32 additive linear mixed-effects models relating flood-disturbance forcing to changes in aquatic-organism indicators before and after floods; Table S6: Interaction linear mixed-effects models comparing the relationships between flood-disturbance forcing and biological responses in the June and August flood events; Table S7: Model diagnostics for the 10 primary additive linear mixed-effects models; Table S8: Sensitivity of regression coefficients in the 10 primary models to river effects, data exclusions, and robust estimation; Table S9: Sensitivity of primary linear mixed-effects model coefficients to threshold settings; Table S10: Proportions of displaced painted-gravel tracers during the June and August 2024 flood events.

Author Contributions: Conceptualization, K.H. and M.H.; methodology, K.H. and M.H.; validation, K.H.; formal analysis, K.H.; investigation, K.H.; resources, M.H.; data curation, K.H.; writing—original draft preparation, K.H.; writing—review and editing, M.H.; visualization, K.H.; supervision, K.H.; project administration, K.H.; funding acquisition, K.H. and M.H. All authors have read and agreed to the published version of the manuscript.

Funding: This research was supported by the River Fund of The River Foundation, Japan (grant number 2024-5311-025), and JSPS KAKENHI (grant number JP23K28277). The research was funded by Dainichi Consultant Inc.

Institutional Review Board Statement: Ethical review and approval were not required for this study under the Animal Experimentation Regulations of Gifu University (Articles 2 and 3). Fish were investigated non-invasively through environmental DNA analysis of river water samples, while benthic macroinvertebrates were collected through standard field sampling for taxonomic identification. No animal experiments requiring ethical approval under these regulations were conducted.

Data Availability Statement: The article and Supplementary Materials provide the original biological data used to calculate percentage changes, the LDA and HDA proportions used in the 10 primary models, and the results of all 32 additive linear mixed-effects models. The individual forcing-proportion values used in the 22 supplementary models are not included in the published materials but are available from the corresponding author upon reasonable request. The underlying data from the two-dimensional depth-averaged flow modeling are also available from the corresponding author upon reasonable request.

Acknowledgments: The authors thank Shigeya Nagayama of Nagano University for his advice on the environmental DNA analysis. The authors also thank Koji Tojo of Shinshu University, Masaki Takenaka of the University of Tsukuba, and Seiya Okamoto of the Aqua Restoration Research Center, Public Works Research Institute, for valuable discussions and comments on the research design and interpretation of the benthic macroinvertebrate results. Part of the DNA extraction and quantitative metabarcoding analyses was conducted by the Research Center of Environmental DNA, Yamaguchi University. The authors also thank the anonymous reviewers for their constructive comments and suggestions, which helped improve the quality and clarity of the manuscript. During the preparation and revision of this manuscript, the authors used ChatGPT (OpenAI) to assist with English translation, language editing, manuscript organization, development of R code for statistical analyses, and preparation of figures and tables. The authors reviewed and verified the AI-assisted outputs and take full responsibility for the content of this publication.

Conflicts of Interest: Author Koji Hijikata was employed by the company Dainichi Consultant Inc. The authors declare that this study received funding from Dainichi Consultant Inc. The funder was not involved in the study design, collection, analysis, interpretation of data, the writing of this article or the decision to submit it for publication.

References

1. Poff, N.L.; Allan, J.D.; Bain, M.B.; Karr, J.R.; Prestegaard, K.L.; Richter, B.D.; Sparks, R.E.; Stromberg, J.C. The natural flow regime: A paradigm for river conservation and restoration. *BioScience* **1997**, *47*, 769–784. https://doi.org/10.2307/1313099.
2. Lytle, D.A.; Poff, N.L. Adaptation to natural flow regimes. *Trends Ecol. Evol.* **2004**, *19*, 94–100. https://doi.org/10.1016/j.tree.2003.10.002.
3. McMullen, L.E.; Lytle, D.A. Quantifying invertebrate resistance to floods: A global-scale meta-analysis. *Ecol. Appl.* **2012**, *22*, 2164–2175. https://doi.org/10.1890/11-1650.1.
4. Gibbins, C.N.; Batalla, R.J.; Vericat, D. Invertebrate drift and benthic exhaustion during disturbance: Response of mayflies (Ephemeroptera) to increasing shear stress and river-bed instability. *River Res. Appl.* **2010**, *26*, 499–511. https://doi.org/10.1002/rra.1282.
5. Lancaster, J.; Hildrew, A.G. Characterizing in-stream flow refugia. *Can. J. Fish. Aquat. Sci.* **1993**, *50*, 1663–1675. https://doi.org/10.1139/f93-187.
6. Matthaei, C.D.; Peacock, K.A.; Townsend, C.R. Patchy surface stone movement during disturbance in a New Zealand stream and its potential significance for the fauna. *Limnol. Oceanogr.* **1999**, *44*, 1091–1102. https://doi.org/10.4319/lo.1999.44.4.1091.
7. Negishi, J.N.; Inoue, M.; Nunokawa, M. Effects of channelisation on stream habitat in relation to a spate and flow refugia for macroinvertebrates in northern Japan. *Freshw. Biol.* **2002**, *47*, 1515–1529. https://doi.org/10.1046/j.1365-2427.2002.00877.x.
8. Sueyoshi, M.; Nakano, D.; Nakamura, F. The relative contributions of refugium types to the persistence of benthic invertebrates in a seasonal snowmelt flood. *Freshw. Biol.* **2014**, *59*, 257–271. https://doi.org/10.1111/fwb.12262.
9. Schwartz, J.S.; Herricks, E.E. Fish use of stage-specific fluvial habitats as refuge patches during a flood in a low-gradient Illinois stream. *Can. J. Fish. Aquat. Sci.* **2005**, *62*, 1540–1552. https://doi.org/10.1139/f05-060.
10. Scott, M.K.; Magoulick, D.D. Swimming performance of five warmwater stream fish species. *Trans. Am. Fish. Soc.* **2008**, *137*, 209–215. https://doi.org/10.1577/T06-278.1.
11. Harada, M.; Nagayama, S. Impacts of flood disturbance on the dynamics of basin-scale swimming fish migration in mountainous streams. *Water* **2022**, *14*, 538. https://doi.org/10.3390/w14040538.

12. Muotka, T.; Paavola, R.; Haapala, A.; Novikmec, M.; Laasonen, P. Long-term recovery of stream habitat structure and benthic invertebrate communities from in-stream restoration. *Biol. Conserv.* **2002**, *105*, 243–253. https://doi.org/10.1016/S0006-3207(01)00202-6.
13. Lepori, F.; Palm, D.; Brännäs, E.; Malmqvist, B. Does restoration of structural heterogeneity in streams enhance fish and macroinvertebrate diversity? *Ecol. Appl.* **2005**, *15*, 2060–2071. https://doi.org/10.1890/04-1372.
14. Hischier, C.M.; Bätz, N.; Rachelly, C.; Demuth, P.; Weitbrecht, V.; Vetsch, D.F.; Dinkel, C.; Weber, C. From habitat heterogeneity to flood refugia: Linking flow intensity and morphology to inform river management. *Sci. Total Environ.* **2026**, *1018*, 181484. https://doi.org/10.1016/j.scitotenv.2026.181484.
15. Harada, M.; Fujita, Y. Considerations on changes in designs of cross-section and roughness in improvement works of small and medium-sized rivers. *J. Jpn. Soc. Civ. Eng. Ser. B1 (Hydraul. Eng.)* **2012**, *68*, I_1291–I_1296. https://doi.org/10.2208/jscejhe.68.I_1291. (In Japanese)
16. Oishi, T.; Takaoka, H.; Harada, M.; Kayaba, Y. The effect of river regulation on channel form in small and medium-sized rivers. *J. Jpn. Soc. Civ. Eng. Ser. B1 (Hydraul. Eng.)* **2014**, *70*, I_997–I_1002. https://doi.org/10.2208/jscejhe.70.I_997. (In Japanese)
17. Nagayama, S.; Harada, M.; Kayaba, Y. Classification of morphology and habitat in streams and rivers: Application to river management. *Ecol. Civ. Eng.* **2015**, *18*, 19–33. https://doi.org/10.3825/ece.18.19. (In Japanese)
18. Japan Meteorological Agency. *Weather in June 2024*; Japan Meteorological Agency: Tokyo, Japan, 2024. (In Japanese)
19. Japan Meteorological Agency. *Heavy Rain, Strong Winds, and Gusts Caused by Typhoon No. 10 in 2024, 27 August–1 September 2024*; Japan Meteorological Agency: Tokyo, Japan, 2024. (In Japanese)
20. Kawai, T.; Tanida, K. (Eds.) *Aquatic Insects of Japan: Manual with Keys and Illustrations*, 2nd ed.; Tokai University Press: Hadano, Japan, 2018. (In Japanese)
21. Takemon, Y. Life-type concept and functional feeding groups of benthos communities as indicators of lotic ecosystem conditions. *Jpn. J. Ecol.* **2005**, *55*, 189–197. https://doi.org/10.18960/seitai.55.1_189. (In Japanese)
22. Ushio, M.; Murakami, H.; Masuda, R.; Sado, T.; Miya, M.; Sakurai, S.; Yamanaka, H.; Minamoto, T.; Kondoh, M. Quantitative monitoring of multispecies fish environmental DNA using high-throughput sequencing. *Metabarcoding Metagenomics* **2018**, *2*, e23297. https://doi.org/10.3897/mbmg.2.23297.
23. Biodiversity Center of Japan, Ministry of the Environment. *A Survey Manual for Conducting eDNA Analysis on Freshwater Fish*, 3rd ed.; Ministry of the Environment: Fujiyoshida, Japan, 2023. (In Japanese)
24. Hirose, T.; Nakamura, N. (Eds.) *Design of Fishways*; Sankaido: Tokyo, Japan, 1991. (In Japanese)
25. Suzuki, O. Endurance swimming speeds of fresh water fish. *J. Jpn. Soc. Civ. Eng.* **1999**, *622*, 107–115. https://doi.org/10.2208/jscej.1999.622_107. (In Japanese)
26. Onitsuka, K.; Akiyama, J.; Yamamoto, A.; Watanabe, T.; Waki, T. Study on burst speed of several fishes living in rivers. *J. Jpn. Soc. Civ. Eng. Ser. B* **2009**, *65*, 296–307. https://doi.org/10.2208/jscejb.65.296. (In Japanese)
27. Yates, M.C.; Cristescu, M.E.; Derry, A.M. Integrating physiology and environmental dynamics to operationalize environmental DNA (eDNA) as a means to monitor freshwater macro-organism abundance. *Mol. Ecol.* **2021**, *30*, 6531–6550. https://doi.org/10.1111/mec.16202.
28. iRIC Project. Nays2DH. Available online: https://i-ric.org/en/solvers/nays2dh/ (accessed on 7 October 2026).
29. Townsend, C.R.; Scarsbrook, M.R.; Dolédec, S. Quantifying disturbance in streams: Alternative measures of disturbance in relation to macroinvertebrate species traits and species richness. *J. North Am. Benthol. Soc.* **1997**, *16*, 531–544. https://doi.org/10.2307/1468142.
30. Mori, T.; Murakami, M.; Saitoh, T. Latitudinal gradients in stream invertebrate assemblages at a regional scale on Hokkaido Island, Japan. *Freshw. Biol.* **2010**, *55*, 1520–1532. https://doi.org/10.1111/j.1365-2427.2009.02363.x.
31. Iwagaki, Y. (I) Hydrodynamical study on critical tractive force. *Trans. Jpn. Soc. Civ. Eng.* **1956**, *41*, 1–21. https://doi.org/10.2208/jscej1949.1956.41_1. (In Japanese)
32. Japan Institute of Country-ology and Engineering. *Guidebook for Channel Planning*; Japan Institute of Country-ology and Engineering: Tokyo, Japan, 2002. (In Japanese)
33. Shimizu, Y.; Kobatake, S.; Arafune, T. Numerical study on the flood-flow stage in gravel-bed river with the excessive reverine trees. *Proc. Hydraul. Eng.* **2000**, *44*, 819–824. https://doi.org/10.2208/prohe.44.819. (In Japanese)
34. Einstein, H.A. *The Bed-Load Function for Sediment Transportation in Open Channel Flows*; Technical Bulletin No. 1026; U.S. Department of Agriculture, Soil Conservation Service: Washington, DC, USA, 1950.
35. Harada, M.; Nagayama, S.; Kawaguchi, Y.; Kayaba, Y. The importance of river confluences as inter-levee floodplain of small and medium-sized rivers. *Ecol. Civ. Eng.* **2020**, *23*, 109–115. https://doi.org/10.3825/ece.23.109. (In Japanese)

36. R Core Team. *R: A Language and Environment for Statistical Computing*; R Foundation for Statistical Computing: Vienna, Austria, 2025.
37. Sagawa, S.; Kayaba, Y.; Akino, J.; Aoki, S.; Omori, T. Characteristics of fish refuge habitats during high flows in a shortcut channel. *Civ. Eng. J.* **2009**, *51*, 12–15. (In Japanese)
38. Onitsuka, K.; Akiyama, J.; Shishido, A.; Takeda, T. Effects of entrance length of side-pocket in open channel flow on evacuation behaviour of *Zacco platypus* in floods. *J. Jpn. Soc. Civ. Eng. Ser. G (Environ. Res.)* **2016**, *72*, II_143–II_148. https://doi.org/10.2208/jscejer.72.II_143. (In Japanese)
39. Harada, M.; Takaoka, H.; Oishi, T.; Kayaba, Y. Effectiveness of local river widening method in the small and medium-sized rivers of alluvial fans. *Adv. River Eng.* **2015**, *21*, 253–258. https://doi.org/10.11532/river.21.0_253. (In Japanese)

Disclaimer/Publisher's Note: The statements, opinions and data contained in all publications are solely those of the individual author(s) and contributor(s) and not of MDPI and/or the editor(s). MDPI and/or the editor(s) disclaim responsibility for any injury to people or property resulting from any ideas, methods, instructions or products referred to in the content.